

## ORIGINAL ARTICLE

# Novel Thiazole-Based Compounds as Potential Beta-Site Amyloid Precursor Protein Cleaving Enzyme 1 Inhibitors for Alzheimer's Disease

Majid Alhomrani <sup>1,2</sup>, Abdulhakeem S. Alamri <sup>1,2</sup>, Walaa F. Alsanie <sup>1,2</sup>, Abdulaziz Alsharif <sup>1</sup>, Osama Abdulaziz <sup>1</sup>, Magdi M. Salih <sup>1</sup>, Bassem M. Rafat <sup>3</sup>, Abdulwhab Alamri <sup>4</sup>, Tahir A. Chohan <sup>5</sup>

<sup>1</sup> Department of Clinical Laboratory Sciences, The Faculty of Applied Medical Sciences, Taif University, Taif, Saudi Arabia

<sup>2</sup> Research Center for Health Sciences, Taif University, Taif, Saudi Arabia

<sup>3</sup> Department of Radiology Sciences, The Faculty of Applied Medical Sciences, Taif University, Taif, Saudi Arabia

<sup>4</sup> Department of Pharmacology and Toxicology, College of Pharmacy, University of Hail, Hail, Saudi Arabia

<sup>5</sup> Institute of Pharmaceutical Sciences (IPS), University of Veterinary & Animal Sciences (UVAS), Lahore, Pakistan

## SUMMARY

**Background:** Alzheimer's disease is a neurodegenerative disorder that causes significant cognitive impairment and memory loss. It is the leading cause of dementia on a global scale and is distinguished by the pathological build-up of amyloid-beta peptides and tau protein. This study presents the development of E-pharmacophore modeling, which utilizes reported co-crystal structure involving beta-site amyloid precursor protein cleaving enzyme 1 (BACE1) to screen the eMolecules database.

**Methods:** The present study comprehensively dealt with the virtual screening and structure-based prediction of thiazole compounds against BACE1 protein. To investigate the binding mode of virtual-screened hits (VS-hits), top 100 VS-hits were docked into BACE1 followed by *in silico* ADMET prediction. Top two VS-hits (CP1 and CP2) with highest docking scores along with co-crystallized ligand (CPZ) were further subjected to MESP, HOMO, LUMO, MD simulation, and MMGBSA analysis to inspect the dynamic stability of inhibitor-BACE1 complexes and the key molecular interaction responsible for their improved binding affinity toward BACE1.

**Results:** This research identified CP1 and CP2 as top two potential novel BACE1 inhibitors from the library of natural products, whose Glide docking scores range from -8.87 to -7.89 kcal/mol<sup>-1</sup>. Interestingly, both ligands were able to establish interactions with a set of conserved residues F108, I110, I118, L30, Q12, G13, G11, A335, S229, D228, G230, D32, G34, S35, and Y71. ADMET assessment of the selected compounds was also noted to be within acceptable ranges. The preliminary *in-silico* ADMET evaluation revealed encouraging results for all the modeled and in-house library compounds. The RMSD and RMSF analysis revealed that both ligands remained stable and maintained their interaction throughout the simulation time (100 nanoseconds). The MM/GBSA (ranging from -36.734 to -27.431 kcal/mol) predicted binding affinities are in strong correlation with that of the docking score, which not only supports the docking results but also suggests that CP1 exhibits superior binding affinity towards BACE1.

**Conclusions:** Keeping in view these findings, CP1 might be a promising candidate for drug discovery against BACE1 inhibitors. The findings of this research have the potential to offer valuable recommendations for the advancement of novel, potent, and efficacious BACE1 inhibitors.

(Clin. Lab. 2025;71:1-18. DOI: 10.7754/Clin.Lab.2025.241234)

### Correspondence:

Abdulhakeem S. Alamri  
Department of Clinical Laboratory Sciences  
The Faculty of Applied Medical Sciences  
Taif University  
Taif  
Saudi Arabia  
Email: a.alamri@tu.edu.sa

Tahir A. Chohan  
Institute of Pharmaceutical Sciences (IPS)  
University of Veterinary & Animal Sciences (UVAS)  
Lahore  
Pakistan  
Email: tahir.chohan@uvas.edu.pk

Manuscript accepted February 10, 2025

## Supplementary Data

### Ligand-based virtual screening (LBVS)

A shape and electrostatics similarity search was conducted using the validated query for ligand-based virtual screening.

### Query validation

The inhibitor bound to the 1TV5 *Pf*DHODH receptor was chosen as the query molecule for use in shape and electrostatics similarity. A query validation run was done using the vROCS program (OpenEye Scientific Software) to determine whether the selected query was suitable for similarity search. The decoys and actives were obtained from the Database of Useful Decoys-Enhanced (DUD-E); <http://dude.docking.org/target/pyrd>. The databases of decoys and actives in the validation helped establish whether the query was chosen to differentiate between the already known active and inactive (decoys) molecules against the target protein [1].

The receiver operating characteristic curve (ROC curve), together with its area under the curve (AUC) and the early enrichment values, are the statistical metrics generated by the vROCS program (OpenEye Scientific Software) that were used to validate the query. The validated question was then used in ligand-based virtual screening of the chromones, chromanones, and chalcones to conduct shape matching and electrostatic similarity searches.

### Shape similarity search

By using the validated query, vROCS (OpenEye Scientific Software) performed a shape similarity search. As generated by the Omega program, the 3D conformers of the ligands were overlaid on the query using the vROCS program, which employs the Gaussian shape overlap to score the ligands. The ligands are scored based on shape (Shape Tanimoto score) and color (Color Tanimoto score) and ranked based on the Tanimoto Combo score (shape and color) [1].

### Electrostatics similarity search

By using the validated query, electrostatics similarity studies on 3D conformers of the ligands were done using EON (OpenEye Scientific Software). EON aligns molecules on the query and calculates the electrostatic potential using the Poisson-Boltzmann and Coulombic electrostatics tools.

The molecules are scored regarding Poisson-Boltzmann electrostatics Tanimoto (ET<sub>pb</sub>), Coulombic electrostatics Tanimoto (ET<sub>pb</sub>), and EON shape Tanimoto (EON\_shape\_tani). The ligands were then ranked using electrostatics Tanimoto combo (ET\_combo), a combination of EON shape Tanimoto and Poisson-Boltzmann electrostatics Tanimoto (ET<sub>pb</sub>) [1].

### Molecular docking with MOE

Docking simulations were also carried out using a Moe-Dock module with an MMFF94x force field (Chemical Computing Group Inc., Montreal, QC, Canada). The selection of the same active site amino acid residues of co-crystal inhibitor was carried out using the site finder module of the MOE program. Dummies atoms were created at the site of selected amino acid residues. The ligand database, which contains VS identified along with the standard inhibitors CPZ of studied protein, was docked into a chosen protein's binding cavity. A docking study was performed with the placement method set to triangular matcher, the scoring methodology to London dG, the refinement methodology to the rigid receptor, and the scoring function to choose the best pose out of 100 poses for each molecule. After completion of the docking protocol, the best poses for each compound were evaluated for their fitting into active pockets, and the best protein-ligand conformations were selected based on the docking score for further analysis.

### DFT studies/MESP/HOMO/LUMO analysis

The Gaussian 09 package (Rev.E.01) with default settings was used for all calculations with B3LYP functional in SVP basis set. Calculating the electronic structure of atoms and molecules is effectively done using this theory. The following information were determined by the current study, i.e. optimized geometric parameters, the frontier molecular orbital (FMO), global and local reactivity descriptors, and molecular electrostatic potential (MEP). Check files were viewed using Gauss view 6.

### MD simulation

MD simulation analyses were performed to predict the ligand binding status in the physiological milieu by incorporating Newton's classical equation of motion [2, 3]. The selected proteins and ligands were optimized and minimized by utilizing Maestro's Protein Preparation Wizard. The steric clashes, bad contacts, and distorted geometries were removed. System Builder tool was employed to build the systems and TIP3P (intermolecular interaction potential 3 points transferable), and an orthorhombic box was used as solvent model having OPLS\_2005 force field [4]. Counter ions were used to neutralize the models and 0.15 M sodium chloride was added to simulate physiological conditions with 300 K temperature and 1 atm pressure throughout the simulation period. For inspection, trajectories were stored after every 100 pico seconds (ps), and protein-ligand stability was confirmed by root-mean-square deviation (RMSD) over time.

### Molecular mechanics and generalized born surface area (MM-GBSA) calculations

By using the OPLS 2005 force field, VSGB solvent model, and rotamer search techniques, the binding free

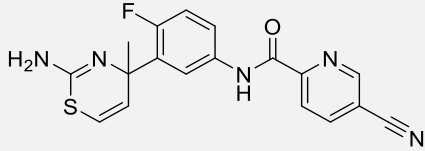
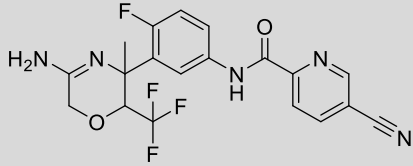
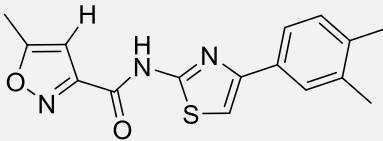
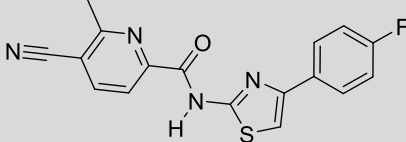
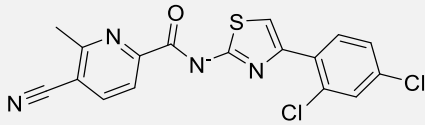
energy was estimated. The MD trajectory frames were chosen at intervals of 10 ns after the MD run. The total free energy binding was calculated using the equation  $\Delta G_{\text{bind}} = G_{\text{complex}} - (G_{\text{protein}} + G_{\text{ligand}})$ , where  $\Delta G_{\text{bind}}$  = binding free energy,  $G_{\text{complex}}$  = free energy of the

complex,  $G_{\text{protein}}$  = free energy of the target protein, and  $G_{\text{ligand}}$  = free energy of the ligand.

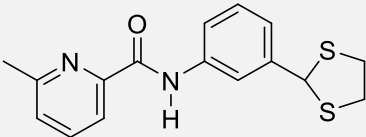
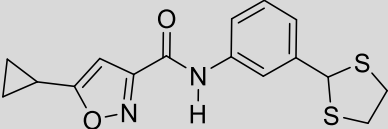
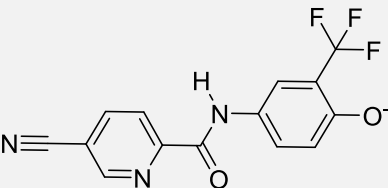
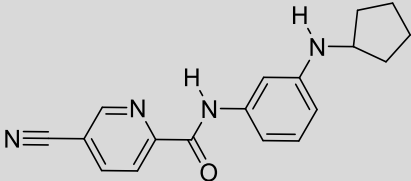
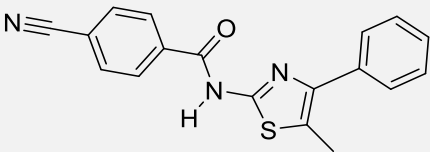
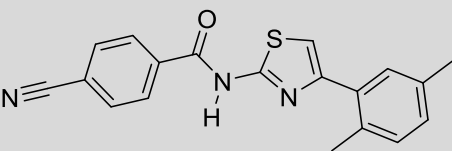
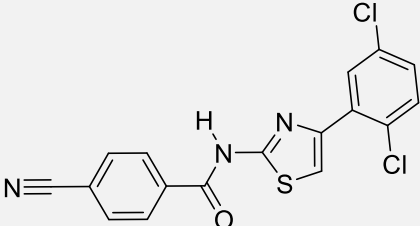
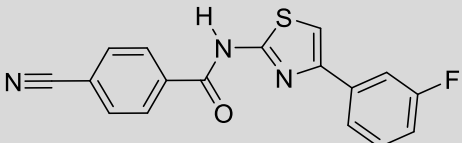
**Table S1.** The area under ROC curves (AUC) and enrichment factor (0.5%, 1%, and 2%) of the 3D virtual screening protocols for selecting query model.

Sr no.	Statistical matrices	Query conformer 2	Query conformer 4	Query conformer 5
ROCS_TanimotoCombo				
1	AUC	0.628	0.656	0.638
2	0.5% enrichment	4.888	14.784	14.068
3	1.0% enrichment	2.453	7.675	7.652
4	2.0% enrichment	2.028	4.044	4.111

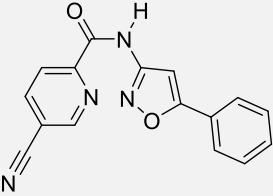
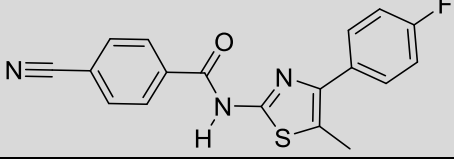
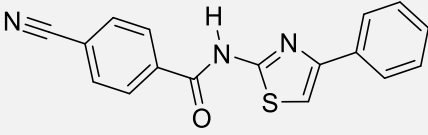
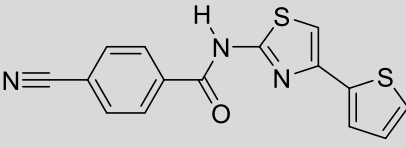
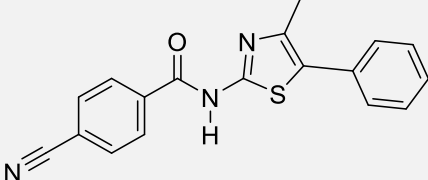
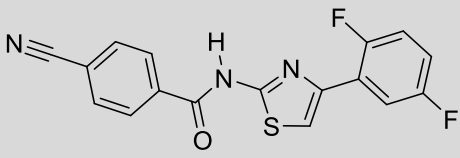
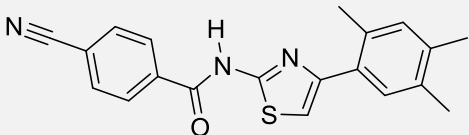
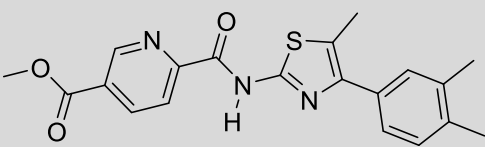
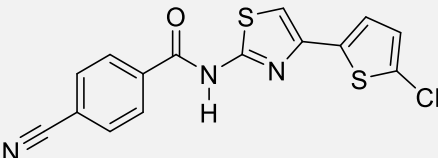
**Table S2.** 2D structures of virtual screening hits along with molecular docking scores for BACE-1 protein by using MOE and Schrödinger-based approach.

Codes	Virtual screen IDs	Structures	MOE docking score	Schrödinger docking score
CPZ	NA		-9.81	-8.87
CP1	106932426_3		-9.04	-7.896
CP2	53756602_1		-8.467	-7.783
CP3	31898758_1		-3.429	-2.893
CP4	30248644_0		-4.862	-3.538

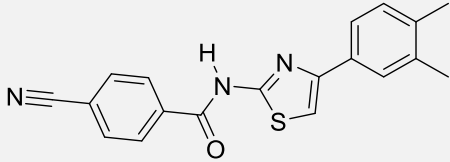
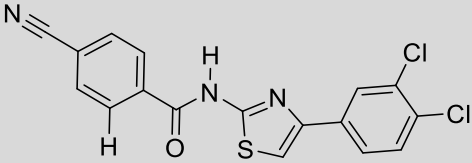
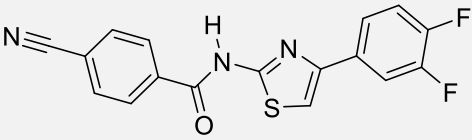
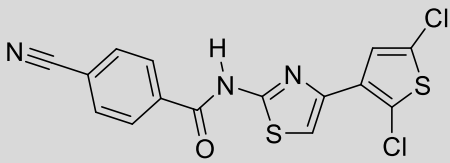
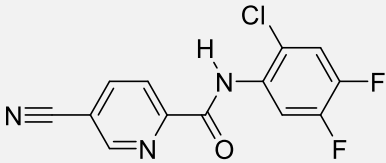
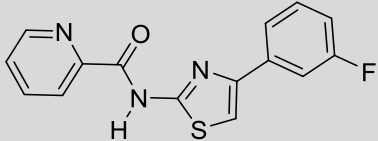
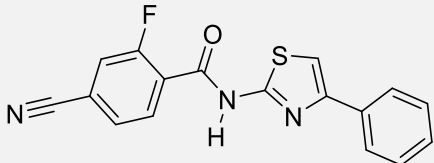
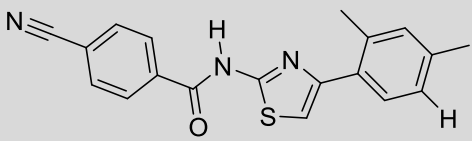
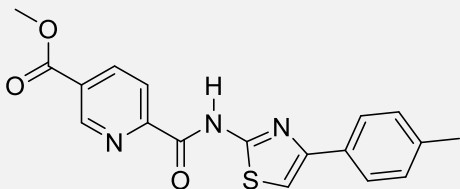
**Table S2. 2D structures of virtual screening hits along with molecular docking scores for BACE-1 protein by using MOE and Schrödinger-based approach (continued).**

Codes	Virtual screen IDs	Structures	MOE docking score	Schrödinger docking score
CP5	24130231_3		-5.18	-4.733
CP6	48209578_6		-4.981	-4.918
CP7	43674956_1		-4.591	-5.703
CP8	49027079_6		-5.703	-4.926
CP9	6162164_1		-4.685	-2.625
CP10	5419252_1		-4.069	-3.417
CP11	2927421_2		-5.868	-4.870
CP12	11906168_4		-4.372	-4.710

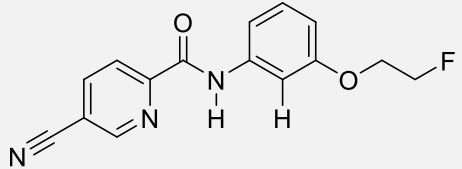
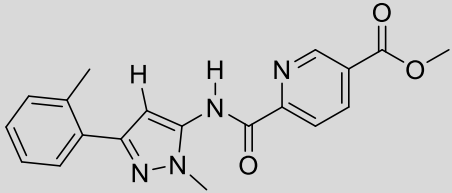
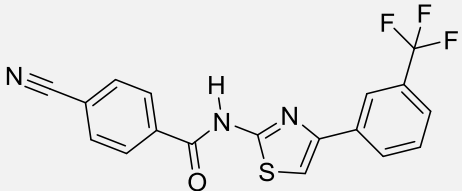
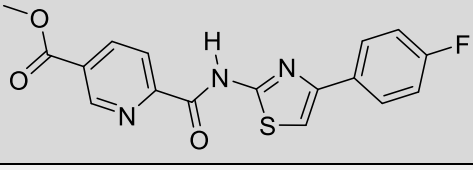
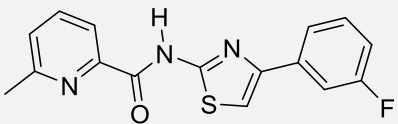
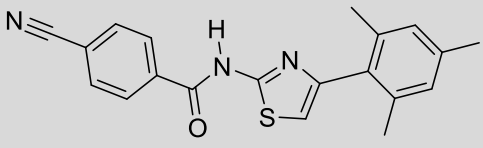
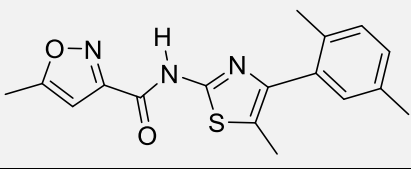
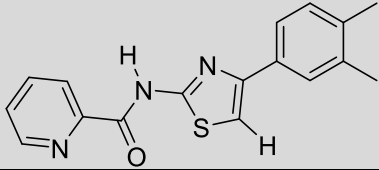
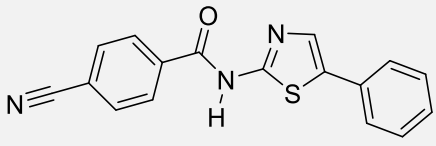
**Table S2.** 2D structures of virtual screening hits along with molecular docking scores for BACE-1 protein by using MOE and Schrödinger-based approach (continued).

Codes	Virtual screen IDs	Structures	MOE docking score	Schrödinger docking score
CP13	49087527_0		-5.321	-3.115
CP14	3353184_1		-5.755	-3.717
CP15	4928879_2		-4.891	-0.055
CP16	2908245_7		-5.649	-5.063
CP17	44093220_4		-4.321	0.875
CP18	43840202_4		-5.149	-3.095
CP19	43843030_1		-4.744	-5.240
CP20	44065400_0		-5.088	-2.771
CP21	2945346_7		-4.861	-4.766

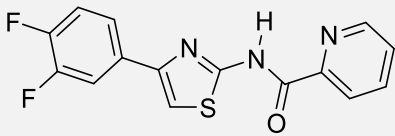
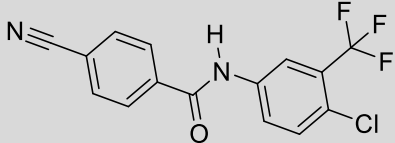
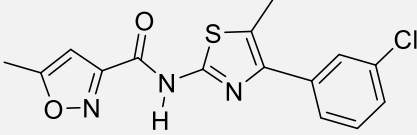
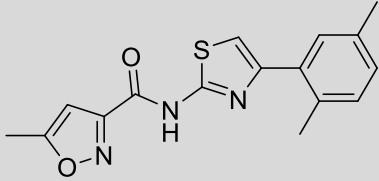
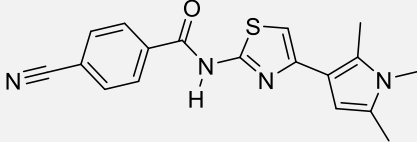
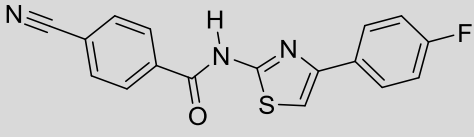
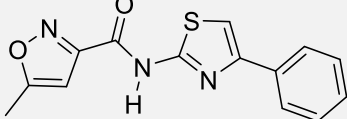
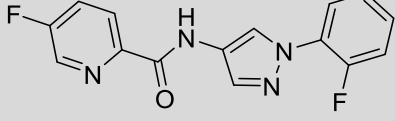
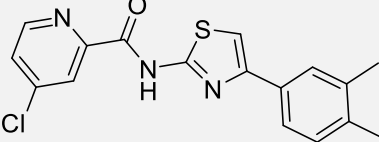
**Table S2. 2D structures of virtual screening hits along with molecular docking scores for BACE-1 protein by using MOE and Schrödinger-based approach (continued).**

Codes	Virtual screen IDs	Structures	MOE docking score	Schrödinger docking score
CP22	4928885_5		-2.086	-3.034
CP23	4928863_5		-4.484	-3.959
CP24	3284649_4		-5.524	-5.043
CP25	17481814_8		-5.013	-4.875
CP26	43399193_0		-3.262	-5.089
CP27	11963322_5		-4.7	-3.710
CP28	2277259_9		-4.207	-2.797
CP29	5419238_1		-5.193	-3.187
CP30	24037746_6		-6.965	-2.715

**Table S2.** 2D structures of virtual screening hits along with molecular docking scores for BACE-1 protein by using MOE and Schrödinger-based approach (continued).

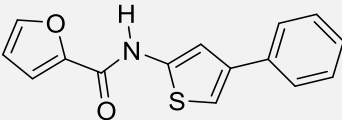
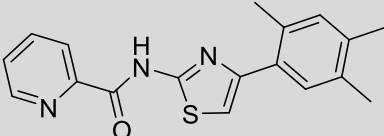
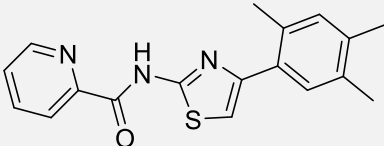
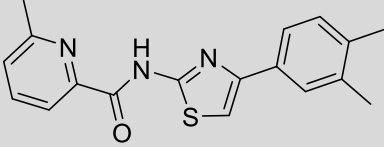
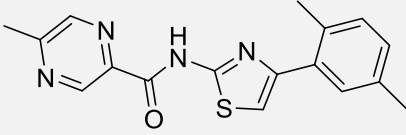
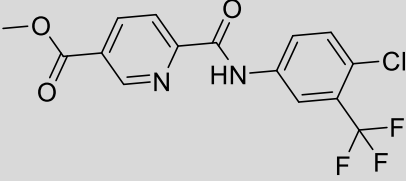
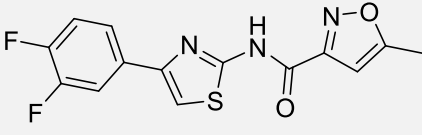
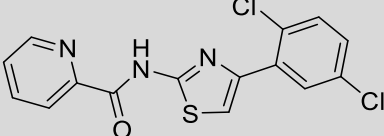
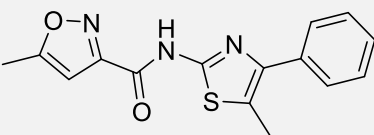
Codes	Virtual screen IDs	Structures	MOE docking score	Schrödinger docking score
CP31	45670113_4		-4.845	-5.015
CP32	53762365_2		-4.511	-2.426
CP33	30005634_8		-5.612	-3.670
CP34	29582998_6		-3.74	-4.414
CP35	33344043_5		-5.354	-5.044
CP36	2930050_0		-1.12	-0.309
CP37	14094390_0		-5.795	-3.900
CP38	43827294_4		0.4784	-4.186
CP39	31912457_5		-5.79	-0.144

**Table S2. 2D structures of virtual screening hits along with molecular docking scores for BACE-1 protein by using MOE and Schrödinger-based approach (continued).**

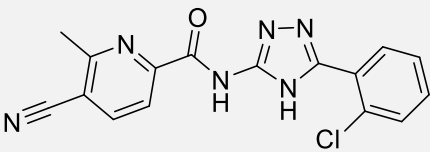
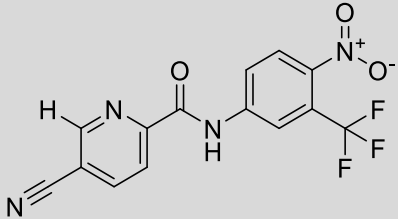
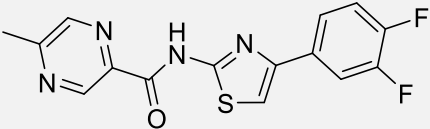
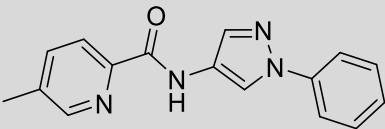
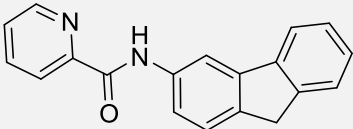
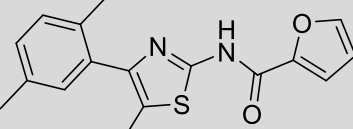
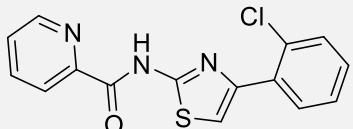
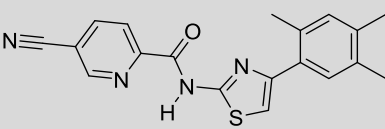
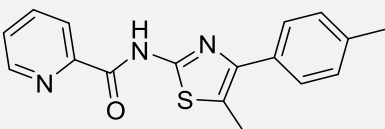
Codes	Virtual screen IDs	Structures	MOE docking score	Schrödinger docking score
CP40	13445610_4		-6.168	-3.918
CP41	3217968_1		-4.736	-5.614
CP42	14095056_0		-4.084	-0.745
CP43	11975256_1		-3.906	-4.035
CP44	3361447_3		-5.286	-4.426
CP45	2927391_0		-4.707	-4.207
CP46	12014446_4		-4.324	-4.081
CP47	53774794_5		-6.471	-4.271
CP48	43919055_4		-4.329	-3.408



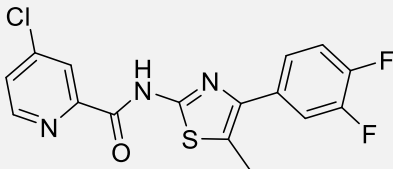
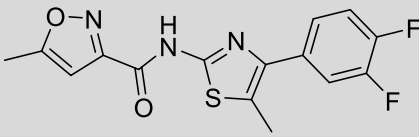
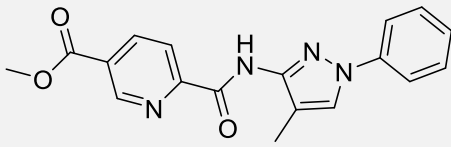
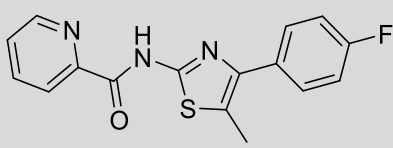
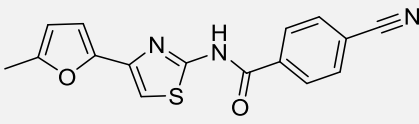
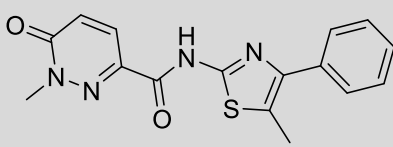
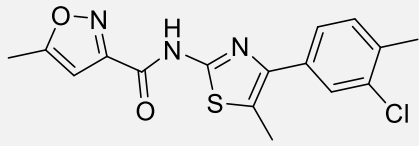
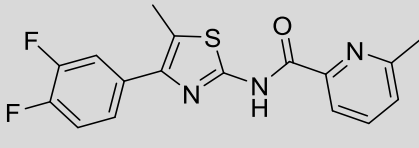
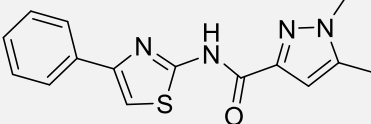
**Table S2.** 2D structures of virtual screening hits along with molecular docking scores for BACE-1 protein by using MOE and Schrödinger-based approach (continued).

Codes	Virtual screen IDs	Structures	MOE docking score	Schrödinger docking score
CP49	3552514_0		-5.599	-4.115
CP50	43843014_1		-5.225	-3.702
CP51	31331838_4		-5.242	-3.681
CP52	44065220_4		-5.591	-3.403
CP53	13452664_1		-5.023	-4.205
CP54	25662152_3		-5.359	-5.330
CP55	24991495_8		-5.788	-4.138
CP56	31312391_0		-5.272	-3.492
CP57	14095098_2		-6.214	-4.058

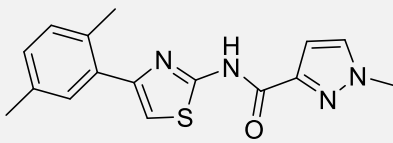
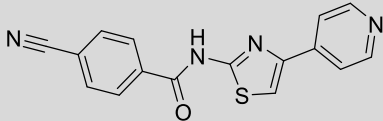
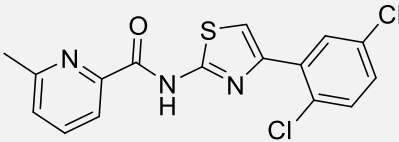
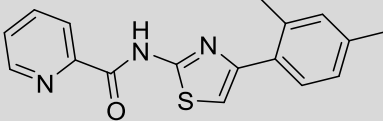
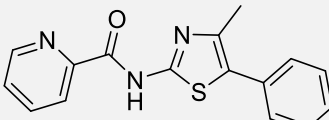
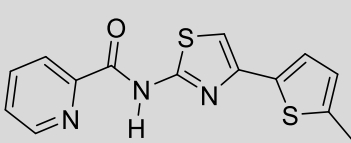
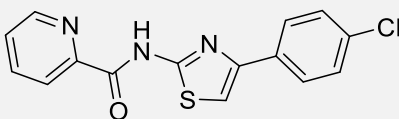
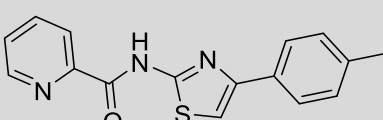
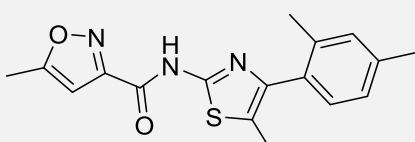
**Table S2. 2D structures of virtual screening hits along with molecular docking scores for BACE-1 protein by using MOE and Schrödinger-based approach (continued).**

Codes	Virtual screen IDs	Structures	MOE docking score	Schrödinger docking score
CP58	36635152_2		-1.851	-3.604
CP59	48827650_1		-6.147	-4.894
CP60	11658298_4		-3.772	-4.235
CP61	53769330_1		-0.03168	-2.496
CP62	3338271_0		-6.222	-4.696
CP63	1317633_0		-4.803	-4.876
CP64	43821173_0		-2.345	-4.619
CP65	14094480_0		-6.86	-4.566
CP66	9866264_0		-5.886	-3.779

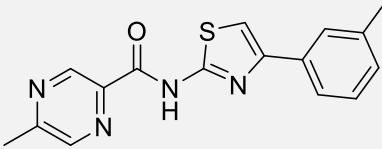
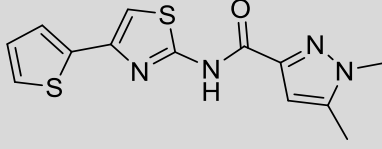
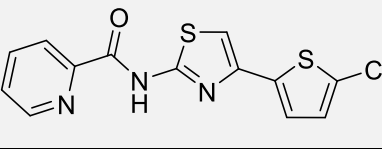
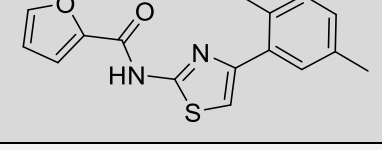
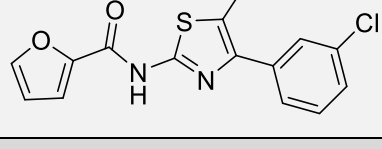
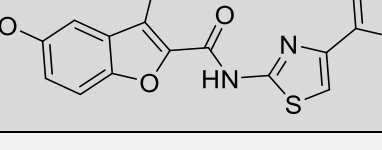
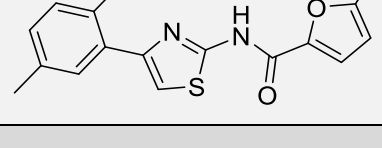
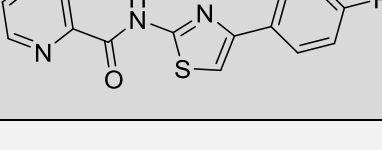
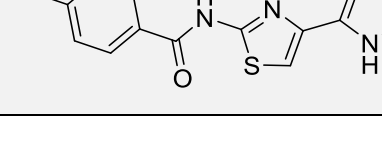
**Table S2.** 2D structures of virtual screening hits along with molecular docking scores for BACE-1 protein by using MOE and Schrödinger-based approach (continued).

Codes	Virtual screen IDs	Structures	MOE docking score	Schrödinger docking score
CP67	43919213_0		-6.307	-4.063
CP68	11979880_0		-5.943	-4.282
CP69	36961239_0		-5.872	-4.838
CP70	10006624_0		-5.445	-3.692
CP71	13516364_6		-4.932	-4.980
CP72	3231693_8		-5.321	-4.321
CP73	1032099_0		-5.594	-4.316
CP74	25662246_0		-4.994	-2.601
CP75	29275285_1		-4.86	-3.527

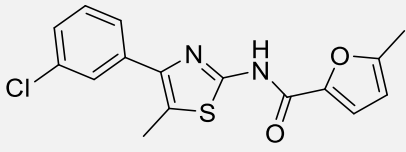
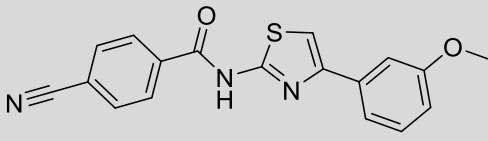
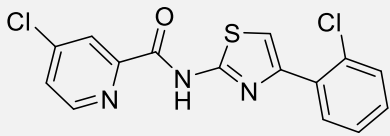
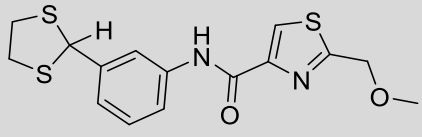
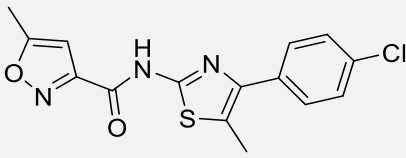
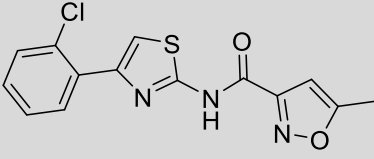
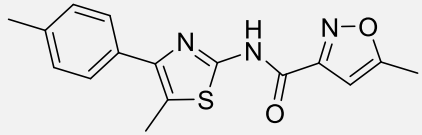
**Table S2. 2D structures of virtual screening hits along with molecular docking scores for BACE-1 protein by using MOE and Schrödinger-based approach (continued).**

Codes	Virtual screen IDs	Structures	MOE docking score	Schrödinger docking score
CP76	16944758_1		-3.175	-3.702
CP77	16826245_2		-4.561	-5.238
CP78	33344017_0		-4.532	-4.200
CP79	43823437_1		-5.248	-4.267
CP80	27410958_7		-5.302	-2.415
CP81	13500205_2		-0.7902	-3.718
CP82	31316163_1		-5.384	-2.831
CP83	9638852_1		-5.396	-3.500
CP84	14094482_1		-4.976	-4.411

**Table S2.** 2D structures of virtual screening hits along with molecular docking scores for BACE-1 protein by using MOE and Schrödinger-based approach (continued).

Codes	Virtual screen IDs	Structures	MOE docking score	Schrödinger docking score
CP85	3026687_1		-6.311	-4.540
CP86	31211140_5		-2.408	-2.041
CP87	3346631_2		-5.578	-4.295
CP88	2515933_1		-2.894	-4.184
CP89	2041644_0		-4.063	-4.741
CP90	3388977_8		-4.715	-2.936
CP91	3998609_1		-6.534	-4.376
CP92	9866246_1		-4.761	-2.553
CP93	17214710_6		-4.372	-4.855

**Table S2. 2D structures of virtual screening hits along with molecular docking scores for BACE-1 protein by using MOE and Schrödinger-based approach (continued).**

Codes	Virtual screen IDs	Structures	MOE docking score	Schrödinger docking score
CP94	14094126_0		-5.804	-5.235
CP95	4950907_8		-5.243	-0.689
CP96	29961425_0		-1.675	-3.878
CP97	48223021_5		-5.725	-5.215
CP98	3672447_0		-6.177	-1.731
CP99	3666277_0		-5.789	-3.663
CP100	14095064_0		-6.486	-3.858

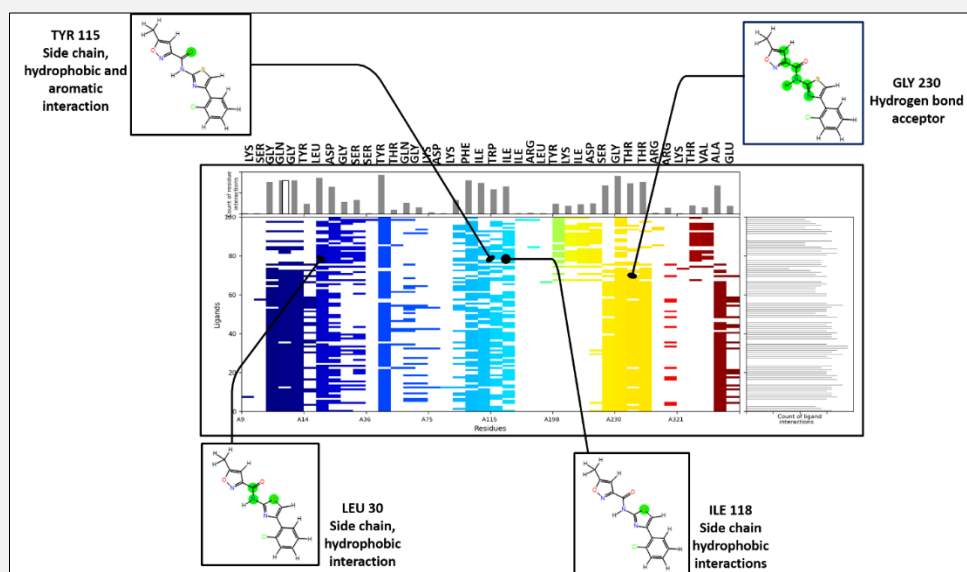


Figure S1. Summary of fingerprint analysis.

Different interactions are shown in different colors along with ligands with highlighted regions involved in various interactions.

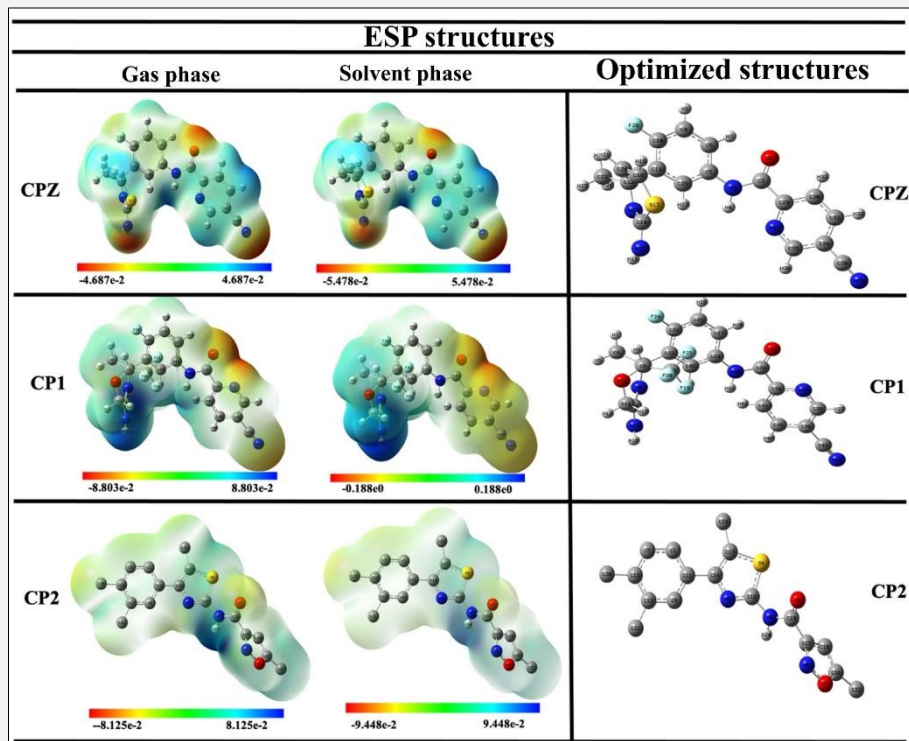


Figure S2. ESP structures (in both gas and solvent phases), formed by mapping of total density over electrostatic potential, and optimized structures.

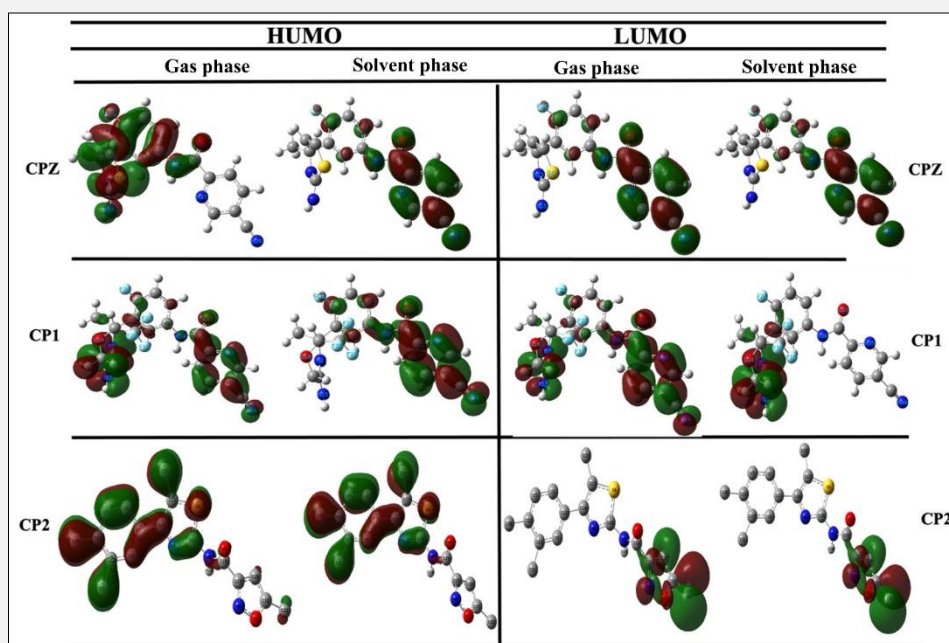


Figure S3. Calculated HOMO and LUMO orbitals of potent derivatives at B3LYP/SVP level of DFT calculations.

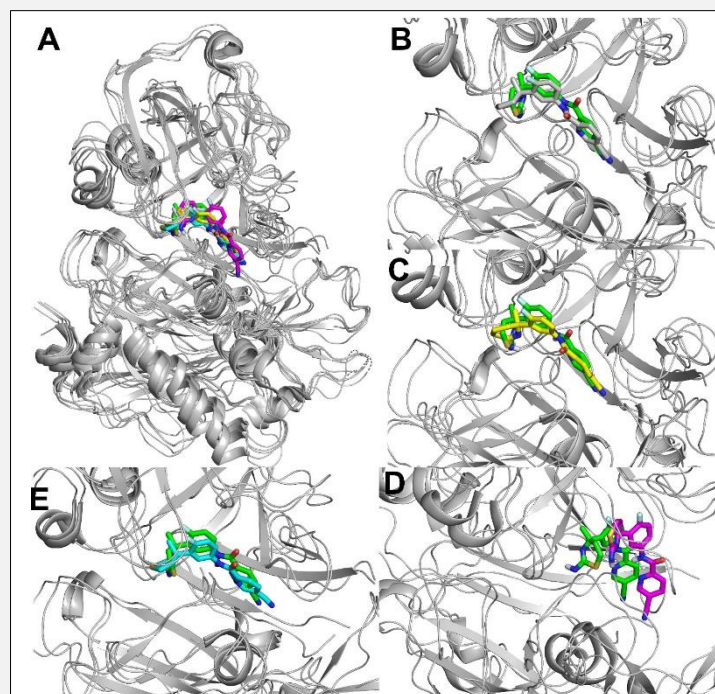
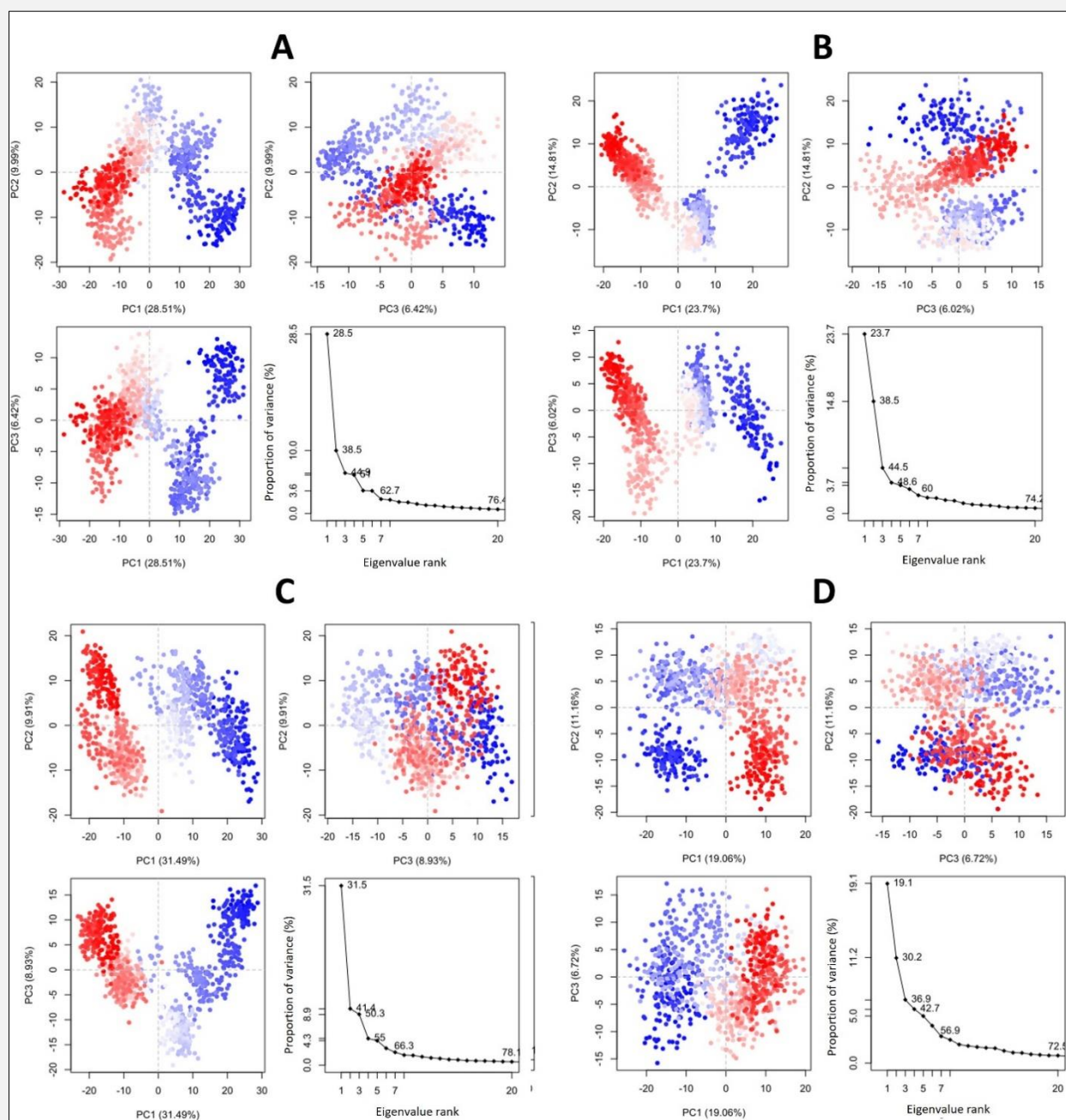


Figure S4. Post-simulated snapshots from MD trajectories of BACE1-CPZ complex extracted from different time points of MD simulation superposed over co-crystallized structure of 7dcz.





**Figure S5. Principal component analysis (PCA) eigenvalue plotted versus the percentage of variance.**

**A - APO-BACE1 protein, B - CPZ-BACE1, C - CP1-BACE1, D - CP2-BACE1.**

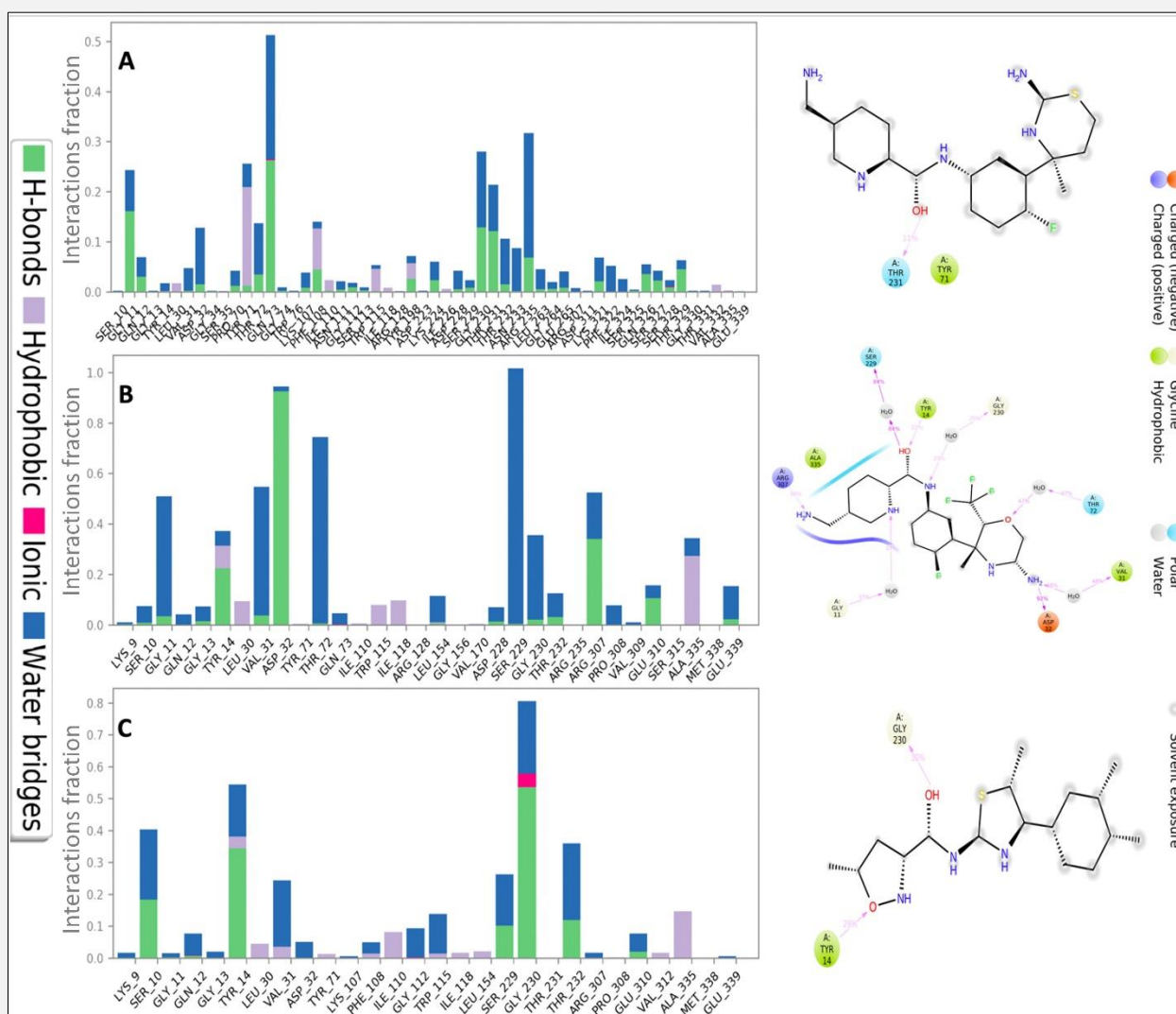


**Figure S6.** Interaction fraction (contact histogram/map) of selected ligands with individual residue in their corresponding complexes BACE1-CPZ (A), BACE1-CP1 (B), and BACE1-CP2 (C) after 100 ns of simulation.

## References:

1. Scolastica M, Ndakala AJ, Derese S. Modeling and synthesis of antiplasmodial chromones, chromanones and chalcones based on natural products of Kenya. *Asian J Nat Prod Biochem* 2018; 16(1):8-21. <https://smujo.id/jnpb/article/view/2505>
2. Hildebrand PW, Rose AS, Tiemann JKS. Bringing molecular dynamics simulation data into view. *Trends Biochem Sci* 2019; 44(11):902-13. (PMID: 31301982)
3. Rasheed MA, Iqbal MN, Saddick S, et al. Identification of lead compounds against Scm (fms10) in *Enterococcus faecium* using computer aided drug designing. *Life* 2021;11(2):77. (PMID: 33494233)
4. Shivakumar D, Harder E, Damm W, Friesner RA, Sherman W. Improving the Prediction of Absolute Solvation Free Energies Using the Next Generation OPLS Force Field. *J Chem Theory Comput* 2010;6(5):1509-19. (PMID: 26592101)